JGR Biogeosciences

RESEARCH ARTICLE
10.1029/2021JG006546

Key Points:

- The typhoon Mangkhut clearly impacted the water column differently on the continental shelf, at the shelf edge and in the deep sea
- On Mangkhut's track a maximum nitrate supply of 162 mmol m^{-2} was caused by induced upwelling at the shelf edge
- The chlorophyll inventory of 2.8 Gg was almost tripled by contributing 4.7 Gg estimated from an additional nutrient supply

Correspondence to:
J. Kuss,
joachim.kuss@io-warnemuende.de

Citation:
Kuss, J., Frazão, H. C., Schulz-Bull, D. E., Zhong, Y., Gao, Y., & Waniek, J. J. (2021). The impact of typhoon "Mangkhut" on surface water nutrient and chlorophyll inventories of the South China Sea in September 2018. *Journal of Geophysical Research: Biogeosciences*, *126*, e2021JG006546. https://doi.org/10.1029/2021JG006546

Received 21 JUL 2021
Accepted 2 DEC 2021

Author Contributions:

Conceptualization: Joachim Kuss, Joanna J. Waniek
Data curation: Yisen Zhong
Formal analysis: Joachim Kuss, Helena C. Frazão, Yisen Zhong, Joanna J. Waniek
Funding acquisition: Detlef E. Schulz-Bull, Joanna J. Waniek
Investigation: Yisen Zhong, Yonghui Gao
Project Administration: Joanna J. Waniek
Supervision: Detlef E. Schulz-Bull
Visualization: Joachim Kuss, Helena C. Frazão, Yisen Zhong

The Impact of Typhoon "Mangkhut" on Surface Water Nutrient and Chlorophyll Inventories of the South China Sea in September 2018

Joachim Kuss[1], Helena C. Frazão[1], Detlef E. Schulz-Bull[1], Yisen Zhong[2], Yonghui Gao[2], and Joanna J. Waniek[1]

[1]Department of Marine Chemistry, Leibniz Institute for Baltic Sea Research Warnemünde, Rostock, Germany, [2]School of Oceanography, Shanghai Jiao Tong University, Institute of Oceanology, Shanghai, China

Abstract The influence of the exceptionally strong typhoon Mangkhut on the availability of nutrients and changes in primary production were studied in the northern South China Sea in September 2018. A tight station grid was sampled to analyze major nutrients, chlorophyll_a, particulate and dissolved organic carbon and nitrogen. Based on interpolated profiles, nutrients and organic matter budgets were determined for the upper 100 m of the water column prior to and after Mangkhut's passage. An upper layer of 100 m was found to reflect the important changes by the typhoon. Considerable differences between the on-shelf, shelf edge and the deep-sea stations were determined. Nitrate and phosphate increased by about 80% and 36% on the shelf, respectively, and both by almost 40% at the shelf edge. The open deep-sea part of the study area reflects some deviating results that may be caused by just displacement of water or by mixing water of different origin. However, right on Mangkhut's track on the shelf even contact between surface waters and bottom waters was enabled, increasing phosphate and silicate, but declining nitrate. The inventory of organic carbon of the upper 100 m of the study area (138,000 km^2) of 92 Gmol had increased within a few days after the typhoon's passage by 5 Gmol on the shelf and about 2 Gmol in the shelf edge area. Chlorophyll_a doubled during our stay and might have reached a factor of 3 increase in the subsequent time by nitrate supply and excess phosphate.

Plain Language Summary The influence of the super typhoon Mangkhut on the waters of the northern South China Sea was studied in September 2018. Nutrients and organic material were measured on 63 stations from the Chinese research vessel HAI YANG DI ZHI SHI HAO. Amounts of nutrients and biogenic matter were calculated for the on-shelf, shelf edge and deep-sea stations for the pre- and post-Mangkhut period. An important finding was that the stations of the different areas, on-shelf, shelf edge and the deep-sea appeared to be differently impacted by Mangkhut. Even differences between the stations right on its track and in the other parts of the study area were found. In general, nutrients were supplied in enormous amounts and caused immediate algae growth. Moreover, enough nutrients were supplied to support algae growth for a couple of weeks. In summary, it was found that Manghut's upper water column mixing and shifting caused an almost tripling of primary production compared to the normal situation.

1. Introduction

A devastating typhoon of category 5 passed the South China Sea (SCS) in September 2018 (Figure 1). Already in the Philippines, it had caused damage as typhoon "Ompong" prior to entering the SCS. Thereafter, it was called typhoon "Mangkhut." It is especially well known in connection with its impact on the region of Hong Kong. The super typhoon brought exceptionally strong winds and severe rainfall (Liu, Wang, et al., 2020) and affected the marine environment by waves and deep mixing (Liu, Li, et al., 2020). Super typhoons are relatively rare and appear up to once or twice in a decade in the studied part of the SCS (Table 1). Enhanced upwelling of deeper waters partly increased salinity and nutrient concentrations, as well reduced the temperature in the surface waters in the range of its path. Whereas increased runoff from coastal sites caused a decrease of surface water salinity at near coastal sites (Liu, Li, et al., 2020) and was accompanied by a supply of nutrients and pollutants (Lo et al., 2020). Major biogeochemical changes with a significant response in the oligotrophic open SCS can be expected. Satellite observation confirmed an increase of near-surface chlorophyll_a concentration the day after the typhoon passage, as water enriched in algae was mixed to the surface (Liu, Li, et al., 2020). Already in 2005, two types of mechanisms were deduced from satellite data that caused phytoplankton blooms in the SCS after a

Writing – original draft: Joachim Kuss, Helena C. Frazão, Detlef E. Schulz-Bull, Yonghui Gao, Joanna J. Waniek

typhoon passage. First, mixing and upwelling indicated by a preceding surface water cooling on the right side of its track and second, a nearshore bloom likely caused by enhanced freshwater drainage and off-shore advection, as the waters showed increased turbidity and colored dissolved organic matter (CDOM) concentrations (Zheng & Tang, 2007). In the Pearl River Estuary (PRE), a cyanobacteria bloom was caused by nutrient supply after typhoon passage (Qiu et al., 2019).

Based on 74 tropical storms (TS) well covered by satellite observation in the SCS, a post-TS increase in chlorophyll_a was shown by satellite ocean color data (Zhao & Wang, 2018). Thereby, chlorophyll_a is significantly correlated with sea surface temperature decrease as an indicator for mixing and upwelling. However, preconditions as the season and the vertical structure of the water are important too (Zhao & Wang, 2018). The impact of Mangkhut on primary production was deduced from satellite data by accounting for Ekman pumping and eddy detection (Liu, Li, et al., 2020). However, in situ sampling and chemical analyses should provide additional information on the changes caused by the category 5 typhoon, since satellite data only provide snapshots of near surface waters and fail to document subsurface conditions and their changes.

The aim of the present study is to characterize the hydrographic and biogeochemical conditions of the northern SCS by means of CTD-O_2 measurements (Waniek, Frazão, et al., 2021) and water sampling with chemical analyses (Waniek, Kuss, et al., 2021). Continuous sensor profiles of temperature, conductivity (salinity) and oxygen were obtained and spatial distributions of nutrients, dissolved and particulate organic carbon and nitrogen, suspended particulate material, chlorophyll_a and phaeopigments were measured on individual water samples to identify changes caused by typhoon Mangkhut. The data were used to estimate typhoon's contribution to biomass production by quantification of nutrient supply and storm-initiated primary productivity in the SCS. We presently do not well understand the effects of super typhoons like Mangkhut on biogeochemical dynamics - and how these might be altered under future climate. Projections for the 21st century suggest that typhoons will expand their reach in an anthropogenically forced northward expansion, although the number of typhoons is expected to remain relatively stable. The intensity of the tropical storms will likely increase, especially for the most intense ones (IPCC, 2019, In press). Hence, the impact on the biogeochemistry of the SCS is herein evaluated in terms of the frequency of the appearance and strength of typhoons and in the context of a globally changing climate.

2. Materials and Methods

The study was conducted in the SCS as part of the Sino-German project MEGAPOL-Megacity's fingerprint in Chinese southern marginal seas. The cruise on the Chinese r/v *Hai Yang Di Zhi Shi Hao* took place from 1st to 27th September 2018. The work was interrupted between 14th in the morning and 18th of September in the evening, because of the passage of the super typhoon Mangkhut.

2.1. Study Area, Sampling, and Analysis Strategy

The station grid (Figure 1a) stretched from the northern shelf of the SCS across the continental slope to the deep SCS (17°–23°N, 112°–117°E). The grid of 63 stations was sampled by CTD casts, of which 44 were sampled prior to Mangkhut, and 19 stations were sampled after Mangkhut's passage (Figure 1a).

We investigated the area spanning from the Pearl River Estuary (PRE) in the southern direction over the northern shelf of SCS, the continental slope toward the deep SCS by a tight station grid. Sampling was done for the analyses of inorganic nutrients nitrate/nitrite, phosphate, and silicate as well as of particulate organic carbon and nitrogen (POC/PON), dissolved organic carbon (DOC), total dissolved nitrogen (TN) from which dissolved organic nitrogen (DON = TN − [nitrate + nitrite]) was calculated, oxygen, chlorophyll_a (chl_a) and suspended particulate material (SPM) (Waniek, Kuss, et al., 2021). The respective 16 FreeFlow water sampling bottles à 10 L and a Seabird SBE 911+ (co. Sea-Bird Scientific) were attached to a rosette system. We used respective duplicate sensor packages for conductivity, temperature and oxygen (Waniek, Frazão, et al., 2021). The chlorophyll-fluorescence and turbidity data were obtained by a fluorometer (ECO FLNT, WET-Labs, Inc.).

We looked at the upper 100 m of the water column, which by inspection was found to have experienced the largest changes during the typhoon passage. Moreover, we separated the study area according to hydrographic regimes into an on-shelf region, a deep-sea part, and the continental slope region. We will show below that the shelf-edge was not only a transition area between shelf and open deep sea but enabled in fact additional upwelling. So, the

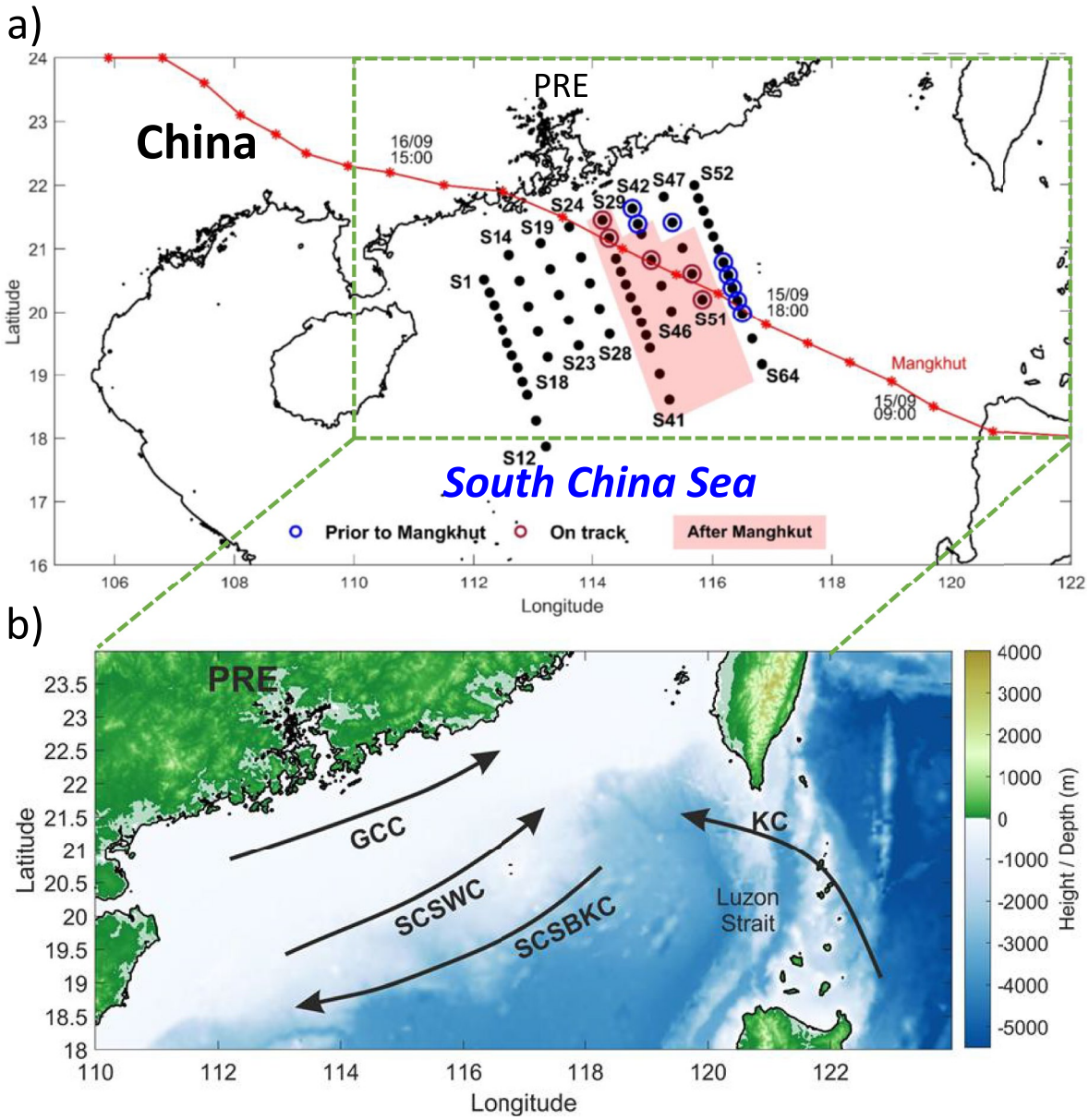

Figure 1. The northern South China Sea with the Pearl River Estuary (PRE). (a) Grid of stations SCS-1 to SCS-12 and SCS-14 to SCS-64 (black dots); stations sampled after the super typhoon Mangkhut are shaded red; stations selected for "on track" evaluation are circled and 6-hourly Mangkhut track positions are represented by red asterisks (CMA Tropical Cyclone Data Center, 2020; Ying et al., 2014). (b) Topography of the study area with dominating currents at the time of the study: Kuroshio Current (KC), Guangdong Coastal Current (GCC), SCS Branch of Kuroshio (SCSBKC), and SCS Warm Current (SCSWC).

changes were often different for the near-coast on-shelf area, the shelf-slope area and the deep-sea environment. Thereby, the grid area of 410 × 335 km could be roughly separated into 44,000 km^2 shelf, 37,000 km^2 shelf edge, and 57,000 km^2 open sea areas. The data set obtained was then analyzed according to stations sampled prior to the Mangkhut passage and afterward. Subsequently, the likely strongest influence of Mangkhut on the water column was elucidated by comparison of on-track stations after the passage of Mangkhut with the situation before its traverse. We determined the average inventories of selected variables and used standard errors to evaluate if observed changes were significant. Thereby, based on interpolated station profiles, averages of respective 10-m-depth intervals were summed to obtain the station inventories of the parameters for the upper 100 m.

Table 1
Total Number of Typhoons Intercepting the Working Area in the Period 1950–2019 as Well as the Number of Typhoons in the Categories Typhoon, Severe Typhoon and Super Typhoon Together With the Average Wind Speed Recorded

	Typhoon		Severe typhoon		Super typhoon		Total typhoon	
Period	Number	Wind (m/s)	Number	Wind (m/s)	Number	Wind (m/s)	Number	Wind (m/s)
1950–1959	11	35.9	3	46.7	2	57.5	16	40.6
1960–1969	12	36.6	9	45.6	1	55	22	40.9
1970–1979	19	35.9	5	46	1	60	25	38.8
1980–1989	10	37	1	45	0	0	11	37.7
1990–1999	12	35.5	2	47.5	0	0	14	37.2
2000–2009	7	33.6	4	46.3	0	0	11	38.2
2010–2019	4	34.8	6	43.5	2	55	12	42.5

2.2. Hydrography

The South China Sea is a large marginal sea of the western Pacific Ocean with an area of 3.5×10^6 km^2 (Huang et al., 1994). The coastal waters of the northern South China Sea (NSCS) are influenced by the drainage of large rivers. Midway along the coast of the sampling area lies the PRE, the Lingdinyang Bay, with the Pearl (Zhujiang) River, one of the largest rivers in China with a highly urbanized catchment area (Figure 1). As a consequence of the high riverine discharges, the coast of the NSCS is nutrient-rich, whereas the open sea basin of the NSCS remains oligotrophic (X. He et al., 2016).

The circulation of SCS is mainly influenced by the prevailing East Asia monsoon (Shaw & Chao, 1994; Wyrtki, 1961), the exchange of water between the SCS and the East China Sea through the Strait of Taiwan, and also between the Kuroshio and SCS in the Strait of Luzon (Hu et al., 2000). During the summer monsoon, when the southwesterly winds prevail, the upper circulation reverses to anticyclonic (Hu et al., 2000). On the shelf of the NSCS, the Guangdong Coastal Current (GCC) is observed (Figure 1b), and it is influenced by the strength of the Pearl River discharge. The GCC is divided at the PRE into the eastern GCC and the western GCC: the eastern GCC flows with the monsoons and enters the ECS through the Taiwan Strait in summer, while the western GCC flows southwesterly along the coast throughout the year (Chen et al., 2019; Huang et al., 1994). However, a strong summer monsoon might reverse the western GCC into a northeastward direction (Huang et al., 1994). The Pearl River Plume is also highly influenced by the prevalent monsoon (Dong et al., 2004). During a strong summer monsoon, the Pearl River Plume might be directed eastwards along the coast, pass the Taiwan Strait and enter into the oligotrophic basin (Bai et al., 2015; X. He et al., 2016; Huang et al., 1994). Further offshore, at the shelf-break region, the northwestward SCS Warm Current (SCSWC) is observed around the 100–200 m isobaths, with maximum intensity in summer (Huang et al., 1994; D. Wang et al., 2014). South of the SCSWC flows a slope current, the South China Sea Branch of Kuroshio (SCSBKC). The SCSBKC is a relatively stable (south-) westward current originating from the Kuroshio Current at the Luzon Strait (Hu et al., 2000; Huang et al., 1994).

2.3. Typhoons

We used the Best Track Data data set from (CMA Tropical Cyclone Data Center, 2020; Ying et al., 2014) and followed the categorization according to the Chinese National Standard for Grade of Tropical Cyclones, which is in use since 15 June 2006, defining typhoons by winds greater than 32.7 m s^{-1} (B. Wang et al., 2007). Thereby, wind speed and precipitable water vapor are closely correlated, as precipitable water vapor is an important property of a typhoon and tropical storms in general, reflecting its energy and strength (Q. He et al., 2020). In total, 111 typhoons crossed the working area between 1950 and 2019 (Figure 2a, Table 1). On a decadal scale, less than 20 typhoons affected the study area, except between 1960–1969 and 1970–1979 (Table 1). Apparently, no clear trend is visible, as is also concluded by the IPCC report (IPCC, 2019, In press).

On an annual scale, the occurrence of typhoons is almost normally distributed, with a gradual increase in the number of events from April to August, reaching a maximum of typhoons in September (Figure 2b). With about 10 typhoons per year cumulating end of summer, it can be expected that the effects of successive typhoons interact.

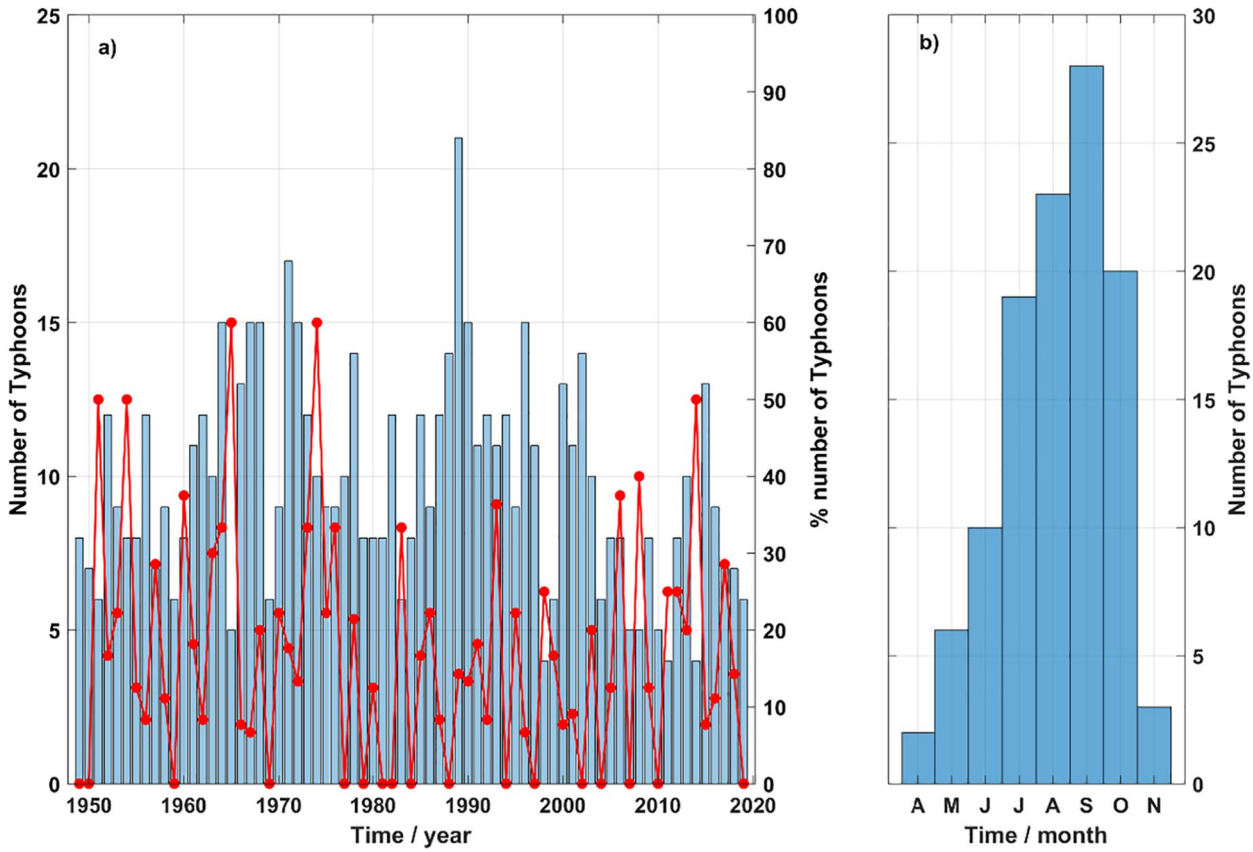

Figure 2. (a) Number of typhoons in the western Pacific region. We used the "Best Track Data" data set (CMA Tropical Cyclone Data Center, 2020; Ying et al., 2014). The blue bars represent the total number of events (per year) in the database, whereas the red line represents the percentage of events that intersected the working area. (b) Average number (1950–2019) of typhoons per month intercepting the working area shown in Figure 1.

So, if a series of typhoons affect the same area, the cold wake of a typhoon causes a weakening of a subsequent typhoon as the temperature decreases by 0.5–1 K (Johnston et al., 2020). Moreover, it is found from a series of typhoons that mixing is increasingly enabled by subsequent typhoons as stratification is reduced. Displacement of the cold wakes by ocean currents over a larger distance may weaken typhoons far away from the previous track.

Mangkhut, a super typhoon, passed the area with wind speeds up to about 50 m s^{-1}. Moreover, the wind speed in the right semicircle of typhoon Mangkhut was clearly higher than in the left semicircle. Mangkhut passed the Philippine Islands with a maximum wind speed of 40 m s^{-1} and a wind stress curl of 1.5×10^{-4} N m^{-3} and notably decreased due to the blockage effect of the Philippine archipelago (X. Liu, Wang, et al., 2020) but reinforced over the SCS again.

2.4. Chemical Analyses

The nutrients nitrate, nitrite, phosphate, and silicate were measured by continuous flow analysis from single samples after return in the IOW home laboratory. The samples were taken on-board and were then immediately filtrated and deep-frozen for final analysis. For quantification, the analytes were converted to colored compounds by wet chemical treatment (Hansen & Koroleff, 1999) and measured with an autoanalyzer (Evolution III, Alliance, Ainring, Germany). Oxygen was measured on one sample of each station by potentiometric Winkler titration (Winkler, 1888) and was used to validate the oxygen sensor registrations. For the unit conversion from measured mL/L to µmol/L we used the O_2 molar volume of 22.3916 L mol^{-1}.

DOC and TN were measured by catalytic oxidation (Cauwet, 1999; Suzuki et al., 1992). Seawater samples were filtered with precombusted GF/F-filters and stored deep frozen until analysis. The samples were acidified and purged to remove inorganic carbon and subsequently injected into the TOC analyzer (TOC-LCPH analyzer,

Shimadzu Deutschland GmbH). We approximate DON as the difference between TN and nitrate/nitrite. The concentration of potentially contributing ammonium to dissolved inorganic nitrogen is virtually zero in oxic waters, as it is immediately taken up after its release.

For analysis of particulate organic carbon and nitrogen (POC, PON), precombusted GF/F-filters were used for sampling and were wetted afterward with hydrochloric acid to remove inorganic carbon (Ehrhardt & Koeve, 1999). The deposits of the dried filters were burned in a Helium atmosphere with oxygen by means of an elemental analyzer (vario MICRO cube, co. Elementar Analysensysteme GmbH). Suspended particulate material (SPM) was sampled on pre-combusted and weighted GF/F-filters (diameter 46 mm, pore size 0.7 µm) and was determined gravimetrically. Chl_a and phaeopigments were measured after ethanol extraction (HELCOM, 2014) of the GF/F filters using a fluorometer (Fluorometer TD10-AU 005, co. Turner Designs).

3. Nutrients and Chlorophyll Concentrations in the Water Column and Their Inventories

Super typhoon's extreme winds and high waves caused clear changes of salinity, temperature, oxygen, nutrients and chlorophyll_a concentrations in upper waters of the SCS. Since the western and the eastern edges of the grid were sampled prior to Mangkhut, these were compared to the central and central-western part of the grid that was sampled after Mangkhut to identify changes in the investigated area of the SCS (Figure 1).

3.1. Changes in the Upper 100 m According to On-Shelf, Shelf Edge, and Deep-Sea Stations

For temperature, a significant increase in the upper 100 m of about 0.61 K on the shelf and 0.67 K above the shelf edge was determined, suggesting that Mangkhut pushed a swell of warmer water in front of it. In contrast, the open sea cooled by 0.42 K because of deeper mixing. However, the simultaneous increase in salinity was significant at the shelf edge only. It amounted to a salinity change of 0.16. This is in agreement with the observation that also oxygen decreased at the shelf edge. It represented a loss of 1.88 mol m^{-2}, corresponding to a decline of 9% in oxygen. These findings show an increased upwelling of deeper waters with higher salinity and lower oxygen concentration. Emission of oxygen could be ruled out as an explanation for the decrease because a loss by gas exchange beyond saturation would not be possible (182 µmol L^{-1} mean value compared to O_2-sat = 205 µmol L^{-1} at $T = 26.48°C$ and $S = 35.93$).

The inventory changes for the parameters are listed in Table 2. For oxygen, nitrate, phosphate, SPM, and chl_a the single station inventories and their changes are additionally shown in Figure 3. It turned out that in the study area, nitrate increased by 42 mmol m^{-2} on the shelf as well as in the slope region in the upper 100 m, contributing about 80% and 40%, to the respective pre-Mangkhut nitrate inventories (Table 2). Phosphate increased by 3.2 mmol m^{-2} (36%) significantly only on the shelf, which includes stations with 80 and 90 m depth. Likely, here near-bottom water is included in the budget (>2 m distance to the seafloor). Similarly, also silicate increased by 94 mmol m^{-2} (34%).

Between 19th and 23rd of September, a few days after the passage of Mangkhut, the algae seemed to have reacted to the nutrient supply. Most dramatic were the changes of chl_a, for which we determined 20 mg m^{-2} on the shelf, 21 mg m^{-2} at the slope and 7 mg m^{-2} in the deep-water region (Table 2). This is between 50% and 100% increase by Mangkhut's additional nutrient supply, after 5–7 days. Interestingly, also SPM increased significantly by 60–70 g m^{-2} on the shelf and its slope but decreased in the open-sea part by 55 g m^{-2}. This might be explained by resuspension in shallow areas of 80–100 m depth and either sedimentation or mixing with less turbid deeper waters in open sea environment, respectively. Particulate organic matter (POC) increased by 15.5% and PON by 21.5% on the shelf (Table 2). From an almost perfect Redfield ratio (Redfield et al., 1963) of the supplied material by showing C:N of 116:18 and no significant contributions of phaeopigments, it can be concluded that it is likely fresh material. Partly degraded material would show carbon enrichment.

3.2. Changes Determined for Stations on Mangkhut's Track

For analyzing the strong local impact of Mangkhut on the sea, we also distinguished on track stations sampled a few days after the passage of Mangkhut with nearby stations sampled before the arrival of Mangkhut as indicated in Figure 1a. On the track, the temperature in the open sea part increased on average in the upper 100 m

Table 2
Inventory Changes in the Water Column in Amounts Per Square Meter and Relative Changes (in Percent) as Well as Average Changes of Temperature and Salinity by Mangkhut in the Upper 100 m of the Water Column (Significant in Bold); for Details See Text

		Balanced changes in the study area		
Parameter	Unit	On-shelf	Shelf edge	Deep sea
Temp	K	**0.61 ± 0.42 (+2.4%)**	**0.67 ± 0.40 (+2.6%)**	**−0.42 ± 0.26 (−1.7%)**
S		0.08 ± 0.14 (+0.2%)	**0.16 ± 0.10 (+0.4%)**	−0.07 ± 0.07 (−0.2%)
Oxygen	mol m^{-2}	0.66 ± 1.03 (+4.0%)	**−1.88 ± 0.91 (−9.4%)**	0.74 ± 0.76 (+4.0%)
PON	mmol m^{-2}	**17.70 ± 7.30 (+21.5%)**	**19.11 ± 8.16 (+28.8%)**	**12.80 ± 8.69 (+19.7%)**
POC	mmol m^{-2}	**115.9 ± 97.7 (+15.5%)**	50.22 ± 85.44 (+8.0%)	**−91.82 ± 46.62 (−14.4%)**
SPM	g m^{-2}	**59.27 ± 29.38 (+49.3%)**	**71.08 ± 33.38 (+76.9%)**	−55.32 ± 57.68 (−34.3%)
Nitrite	mmol m^{-2}	−1.02 ± 5.92 (−5.4%)	0.02 ± 2.61 (+0.1%)	−2.13 ± 3.58 (−14.7%)
Nitrate	mmol m^{-2}	**42.13 ± 16.59 (+81.2%)**	**42.00 ± 31.38 (+39.4%)**	−12.94 ± 70.89 (−5.6%)
Phosphate	mmol m^{-2}	**3.23 ± 1.22 (+35.8%)**	6.08 ± 6.92 (+38.1%)	−5.31 ± 7.57 (−19.2%)
Silicate	mmol m^{-2}	**93.97 ± 27.47 (+33.6%)**	−14.4 ± 109.1 (−3.2%)	−78.6 ± 113.3 (−13.6%)
Chl_a	mg m^{-2}	**20.38 ± 4.32 (+72.7%)**	**21.32 ± 9.30 (+102.9%)**	**7.25 ± 1.70 (+53.0%)**
Phaeopig	mg m^{-2}	4.28 ± 3.78 (+15.1%)	**−7.08 ± 5.46 (−26.0%)**	**3.77 ± 3.03 (+16.8%)**
DOC	mol m^{-2}	0.34 ± 0.52 (+5.7%)	**−0.86 ± 0.29 (−12.6%)**	0.23 ± 0.30 (+3.5%)
DON	mol m^{-2}	**−0.09 ± 0.05 (−15.5%)**	**−0.17 ± 0.03 (−27.8%)**	−0.04 ± 0.07 (−9.8%)
TN	mol m^{-2}	−0.08 ± 0.06 (−11.9%)	**−0.14 ± 0.04 (−18.7%)**	−0.06 ± 0.08 (−9.0%)

by 1.9 K (Table 3). This indicates a swell of warm, oligotrophic water in front of Mangkhut. We also emphasize that the changes observed where Mangkhut passed the shelf edge (Table 3) showed an increase of nitrate of 162 mmol m^{-2}, which reflected almost a doubling. In comparison, silicate increased by 24% (160 mmol m^{-2}), and phosphate decreased by 50% (6.2 mmol m^{-2}). Also, particulate organic nitrogen and carbon increased by 25 mmol m^{-2} (35%) and 134 mmol m^{-2} (25%), respectively. On the shelf, nitrate decreased by 20 mmol m^{-2} (24%), whereas phosphate concentration increased by 10% (1.1 mmol m^{-2}) and silicate by 12% (36.5 mmol m^{-2}) (Table 3). This finding could be explained by upward mixing of near-bottom waters enriched in remineralized nutrients, with a deficit of nitrate indicating denitrification activity close to the sea floor on the shelf. Similarly, also oxygen decreased on the shelf on Mangkhuts track by 5.6%. A study of the coastal transition zone on the northern shelf of SCS close to PRE indicated hypoxia, nitrification and denitrification processes (Li et al., 2020). Chl_a clearly increased on the shelf by 60% (18 mg m^{-2}), at the shelf edge of 58 mg m^{-2} which corresponded to a fourfold increase, and in the deep-sea by 14 mg m^{-2} (~factor of 2) on the track directly impacted by Mangkhut.

4. Discussion of the Inventory Changes On-Shelf, at the Shelf Edge, and in the Open Sea

The study area in the South China Sea appeared relatively homogenous at alongshore currents during the summerly south-west monsoon (Figure 1b). The mixed layer was basically oligotrophic with a weak chl_a maximum between 50 and 80 m depth prior to the typhoon. Indications of waters from the PRE on the off-shore station grid was negligible, even for the stations nearest to the coast. Since the measurements of the second part of the field study were done a few days after the passage of Mangkhut, its impact was ongoing. In the surface ocean around the typhoon path, strong vertical mixing and Ekman upwelling were induced (Liu, Li, et al., 2020). Thereby, Ekman upwelling is a vertical process, which moves high-nutrient subsurface water to the euphotic layer. The wind-induced mixing process redistributes the nutrients over the mixed layer. Biomass was already significantly increased after a few days. A recent study found an immediate increase of chl_a right after a typhoon, just by mixing of chlorophyll from its maximum at depth to the surface (Pan et al., 2017). In our study, we rely on budgets of the upper 100 m that basically excludes such biases and further nutrient supply certainly fostered additional biomass production. So, the organic carbon and nitrogen inventories already had changed a couple of days after

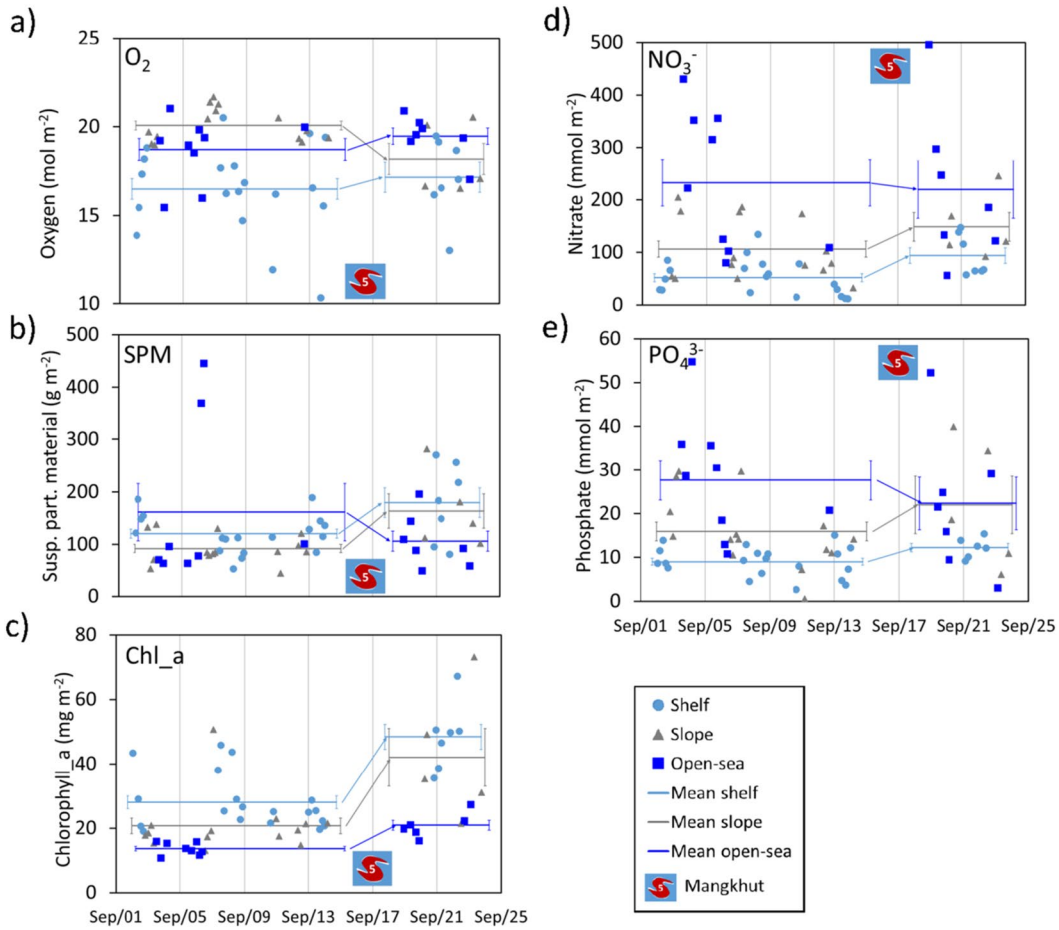

Figure 3. Development of the inventories of selected parameters in the upper 100 m of the water column from prior of Mangkhut appearance to after its passage: on-shelf (light blue dots), the continental slope (gray triangles), and the open-sea regions (blue squares) are distinguished; (a) Oxygen (mol m^{-2}), (b) Suspended particulate material (g m^{-2}), (c) Chlorophyll_a (mg m^{-2}), (d) Nitrate (mmol m^{-2}), and (e) Phosphate (mmol m^{-2}). The quantitative and percentage changes are given in Table 2.

Mangkhut's passage and based on available nitrate and phosphate, a subsequent increase in primary production could be expected. The Redfield ratio (Redfield et al., 1963) reflects a solid basis to estimate biomass, based on the availability or consumption of one of its major components: carbon:nitrogen:phosphorus which is reflected on average by the ratios 115:16:1. This corresponds to a typical C/N ratio of 7.2 mol mol^{-1}. In the study area, we found an average C/N ratio of particulate organic material of 8.7 ± 1.0 mol mol^{-1}, a concentration ratio of dissolved nutrients in the upper 100 m of nitrate to phosphate of 7.5 ± 1.5 mol mol^{-1}. The chlorophyll/carbon ratio, in turn, was 0.063 ± 0.014 g mol^{-1}. These values enabled an estimate of the unused inorganic nutrients at the time of measurement, to be included in the budget (Figure 4, Table 4). Moreover, the phosphate surplus is attributed to biomass production by diazotrophic cyanobacteria, which might have completed the potential biomass production caused by Mangkhut.

The increase of biomass expressed in organic carbon is 116 mmol m^{-2} on the shelf, 50 mmol m^{-2} at the shelf edge and a loss of 92 mmol m^{-2} in the upper 100 m of the studied deep-sea part. This went in parallel with a major nitrate supply of 42 mmol m^{-2}, as well on the shelf as at the shelf edge, and a loss of about 13 mmol m^{-2} in the deep-sea region. Also, phosphate was filled up in upper waters by 3.2 mmol m^{-2} on the shelf, 6.1 mmol m^{-2} at the shelf edge and also showed a loss of 5.3 mmol m^{-2} in the studied open sea area after the typhoon passage. Mangkhut might have pushed some oligotrophic waters from far off-shore closer to the shelf. On the shelf, however, phosphate was slightly in excess of nitrate according to the Redfield ratio, supporting 302 mmol m^{-2} carbon fixation, compared to phosphate, supporting 368 mmol m^{-2} carbon fixation. The slight nitrate deficit might be caused by

Table 3
Inventory Changes in the Water Column on the Track of Mangkhut (in Amounts per Square Meter and Relative Changes in Percent) as Well as Average Changes of Temperature and Salinity in the Upper 100 m of the Water Column (Significant in Bold); for Details See Text

		Balanced changes on Mangkhut's track		
Parameter	Unit	On shelf	Shelf edge	Deep sea
Temp	K	0.40 ± 0.74 (+1.5%)	**0.64 ± 0.15 (+2.5%)**	**1.94 ± 0.23 (+7.5%)**
S		0.29 ± 0.31 (+0.8%)	−0.08 ± 0.03 (−0.2%)	0.07 ± 0.14 (+0.2%)
Oxygen	mol m^{-2}	−0.93 ± 1.57 (−5.6%)	−0.38 ± 0.47 (−1.8%)	−1.36 ± 1.21 (−7.4%)
PON	mmol m^{-2}	**22.3 ± 16.26 (+26.8%)**	**25.5 ± 12.2 (+35.4%)**	**14.50 ± 4.76 (+22.6%)**
POC	mmol m^{-2}	**250 ± 134 (+42.3%)**	**134 ± 67 (+25.0%)**	−89.3 ± 38.7 (−15.1%)
SPM	g m^{-2}	**78.9 ± 40.4 (+111%)**	**58.2 ± 2.9 (+70.9%)**	−239 ± 112 (−80.1%)
Nitrite	mmol m^{-2}	**8.11 ± 5.45 (+82.1%)**	−2.20 ± 1.35 (−22.3%)	−1.49 ± 2.06 (−16.6%)
Nitrate	mmol m^{-2}	−19.58 ± 26.13 (−23.6%)	**162 ± 7 (+195%)**	**19.73 ± 12.98 (+19.2%)**
Phosphate	mmol m^{-2}	**1.08 ± 0.84 (+10.2%)**	−6.18 ± 1.78 (−50.2%)	−11.04 ± 2.29 (−78.1%)
Silicate	mmol m^{-2}	36.5 ± 40.7 (+11.8%)	**159 ± 72 (+24.1%)**	−256 ± 98 (−42.5%)
Chl_a	mg m^{-2}	**17.85 ± 6.54 (+57.5%)**	**58.0 ± 2.1 (+381%)**	**13.9 ± 1.2 (+104%)**
Phaeopig	mg m^{-2}	−3.83 ± 5.31 (−12.4%)	−18.2 ± 0.2 (−99.1%)	−3.70 ± 4.78 (−13.9%)
DOC	mol m^{-2}	0.77 ± 1.30 (+14.2%)	−0.18 ± 0.06 (−2.7%)	−0.26 ± 0.53 (−4.2%)
DON	mol m^{-2}	−0.02 ± 0.08 (−3.9%)	−0.13 ± 0.03 (−23.5%)	−0.24 ± 0.05 (−44.2%)
TN	mol m^{-2}	−0.03 ± 0.07 (−5.5%)	0.03 ± 0.02 (+4.3%)	−0.22 ± 0.06 (−33.7%)

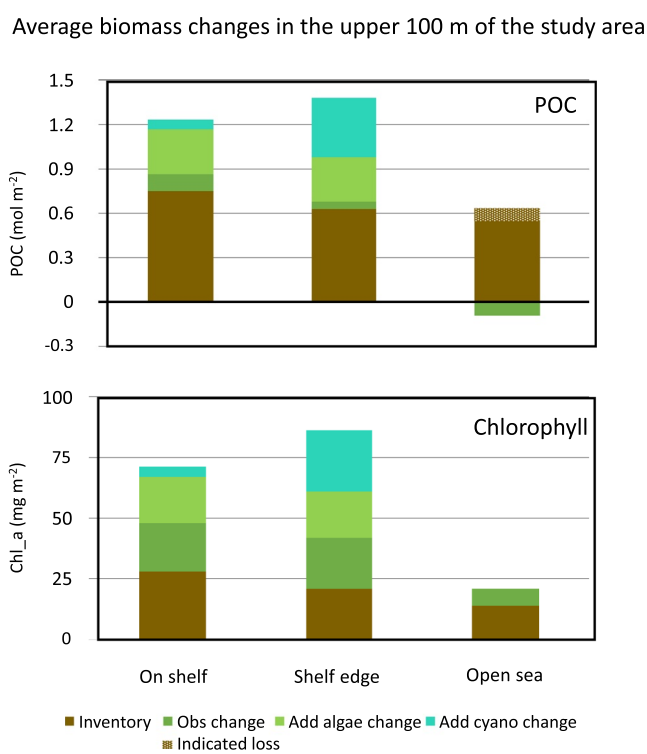

Figure 4. Changes of particulate organic carbon (POC) (upper panel) and chlorophyll_a (lower pane) in the upper 100 m of the study area; Inventories prior to Mangkhut are combined with observed changes (dark green) and expected developments of algae based on nitrate (light green) and of cyanobacteria based on phosphorous surplus (light blue-green). The loss of nitrate and phosphate in the open-sea region was ignored.

mixing with denitrified and phosphate enriched near-bottom waters. It could be expected that the remaining phosphate would be subsequently consumed by diazotrophic cyanobacteria which use dinitrogen gas as a nitrogen source for primary production.

The changes per square metre could then be scaled up by area allocation according to the investigated sites on the shelf, at the shelf edge and in the open deep-sea part of the study area. Before Mankhut, we had a total of 92 Gmol (10^9 mol) organic carbon in the upper 100 m of the study area (Table 4), which had increased a few days after the storm by 5 Gmol on the shelf and about 2 Gmol in the shelf edge region that showed 33 and 23 Gmol, respectively, before. After the typhoon's passage also a decline of POC was observed from 36 Gmol by 5 Gmol in the open sea area. Finally, a POC increase by 2 Gmol in the study area is observed that corresponded to an area-weighted average of a surplus of 12 mmol m^{-2} POC in the upper 100 m of the water column (Table 4). Based on available nitrate, additional 24 Gmol carbon might have been fixed by algae within two to three weeks after the typhoon. Moreover, 18 Gmol carbon could be additionally contributed by diazotrophic cyanobacteria growth, supported by excess phosphate. In terms of chl_a with a stock of 2.8 Gg, which was observed to increase by 2.1 Gg until a few days after Mangkhut's passage, plus potentially 1.5 Gg by algae and additionally 1.1 Gg potentially contributed by cyanobacteria. This reflected almost a doubling during our stay in the area and may have developed to a factor of 2.7 increase of chl_a in the subsequent time after the typhoon in the study area.

The finding of a significant enhancement of primary production in the aftermath of Mangkhut, may give rise to the suggestion that super typhoons might increase oceanic carbon dioxide uptake. However, it has to be considered that the deep mixing of the waters by typhoons not only increase nutrients in the

Table 4
Determined Particulate Organic Carbon (mmol m^{-2}) and Chlorophyll (in mg m^{-2}) Inventories and Changes in the Study Area on the Shelf, at the Shelf Edge, and in the Deep-Sea Areas of the Upper 100 m of the Water Column; per Square Meter and in Gmol (10^9 mol) Organic Carbon and Gg (10^9 g) Chlorophyll by Accounting for the Study Area Size (First Column)

	Inventory before Mangkhut's passage		Observed changes		Estimated potential of change by algae[a]		Estimated potential of change by cyanobacteria[b]	
Particulate organic carbon								
Area/km^2	mmol m^{-2}	Gmol	mmol m^{-2}	Gmol	mmol m^{-2}	Gmol	mmol m^{-2}	Gmol
On shelf/44,000	749	33	116	5	302	13	66	3
Shelf edge/37,000	629	23	50	2	302	11	399	15
Deep sea/57,000	636	36	−92	−5	-	-	-	-
Total study area	670	92	12	2	177	24	128	18
Chlorophyll_a								
	mg m^{-2}	Gg	mg m^{-2}	Gg	mg m^{-2}	Gg	mg m^{-2}	Gg
On shelf/44,000	28	1.2	20	0.9	19	0.8	4	0.2
Shelf edge/37,000	21	0.8	21	0.8	19	0.7	25	0.9
Deep sea/57,000	14	0.8	7	0.4	-	-	-	-
Total study area	20	2.8	15	2.1	11	1.5	8	1.1

Note. The "totals" in per square meter reflect an area-weighted average for the whole study area.
[a]Based on nitrate and phosphate. [b]Based on phosphate residues.

euphotic layer, but also supplies inorganic carbon, especially carbon dioxide to surface waters. This is supported by the oxygen decline that was observed in the shelf edge region (Table 2). Evidence is also provided by a study on typhoons' enhancement of carbon dioxide efflux by 23%–56% in the northern SCS during the last decade (Yu et al., 2020). Likely, the balance would be neither positive nor negative in terms of carbon dioxide uptake, as remineralization would keep the C:N:P ratio of organic matter. So stirring up nutrients that foster primary production would be balanced by respective inorganic carbon. Thus, overall, the additional primary production based on new nutrients likely would not cause additional carbon dioxide uptake. The study area of about 138,000 km^2 represented only 4% of the SCS, so obviously the impact of frequently occurring typhoons in the SCS considerably accelerates the carbon turnover of a vast amount of matter in this marginal sea.

5. Conclusions

Our study area in the northern SCS reflected only 4% of the whole SCS but showed a tremendous turnover of nutrients and matter in the open sea area by the super typhoon Mangkhut. Likely, it mixed and displaced large amounts of water by pushing a swell of warmer water on its front side and subsequently deep mixing by extremely strong winds. The super typhoon caused a special situation that accelerated nutrient mobilization and primary production in a marginal sea of the tropical West Pacific. The globally changing climate likely has little impact on the typhoon activity of the SCS and its biogeochemistry, because only a slight tendency of an increased force of the strong typhoons is expected from climate projections in that area. The major change in typhoon dynamics is a further reach to the North, but this does not account for the SCS, but may affect the tropical and partly the subtropical west Pacific in general.

Data Availability Statement

The data used for this paper are properly cited and referred to in the reference list. CTD data are available at https://doi.pangaea.de/10.1594/PANGAEA.936352. Nutrient data are available at https://doi.pangaea.de/10.1594/PANGAEA.936096.

Acknowledgments
This study was conducted as part of the Sino-German project MEGAPOL funded by the German Federal Ministry of Education and Research (BMBF, Germany) and the State Oceanic Administration (SOA, China). The authors acknowledge the organization of the cruise by Guangzhou Marine Geological Survey (GMGS, China), and the friendly relationship with the scientists and the crew on board. They also thank the technicians for their skillful analytics, especially Lars Kreuzer for nutrients determinations, Jenny Jeschek for organic matter analysis, and Elen Fleckstein for chlorophyll determinations supported by Christian Burmeister (all IOW). They particularly thank the captain and the crew of r/v *Hai Yang Di Zhi Shi Hao* for the excellent co-operation during the cruise and the careful and anticipatory maneuvering of the ship during such an extremely special weather situation. Funding by BMBF of the project "MEGAPOL-Megacity's fingerprint in Chinese southern marginal seas" (grant number: 03F0786A) as well as the financial support of the National Science Foundation of China (Grant No. 41861134040, 41706014) is greatly acknowledged.

References

Bai, Y., Huang, T.-H., He, X., Wang, S.-L., Hsin, Y.-C., Wu, C.-R., et al. (2015). Intrusion of the Pearl River plume into the main channel of the Taiwan Strait in summer. *Journal of Sea Research*, *95*, 1–15. https://doi.org/10.1016/j.seares.2014.10.003

Cauwet, G. (1999). Determination of dissolved organic carbon and nitrogen by high temperature combustion. In K. Grasshoff, K. Kremling, & M. Ehrhardt (Eds.), *Methods of seawater analysis* (pp. 407–420). Wiley-VCH.

Chen, B., Xu, Z., Ya, H., Chen, X., & Xu, M. (2019). Impact of the water input from the eastern Qiongzhou Strait to the Beibu Gulf on Guangxi coastal circulation. *Acta Oceanologica Sinica*, *38*(9), 1–11. https://doi.org/10.1007/s13131-019-1472-2

CMA Tropical Cyclone Data Center. (2020). Tropical Cyclone data center for the western North Pacific basin. In *China meteorological administration*. Shanghai Typhoon Institute. Retrieved from http://tcdata.typhoon.org.cn/en/zjljsjj_sm.html

Dong, L., Su, J., Ah Wong, L., Cao, Z., & Chen, J.-C. (2004). Seasonal variation and dynamics of the Pearl River plume. *Continental Shelf Research*, *24*(16), 1761–1777. https://doi.org/10.1016/j.csr.2004.06.006

Ehrhardt, M., & Koeve, W. (1999). Determination of particulate organic carbon and nitrogen. In K. Grasshoff, K. Kremling, & M. Ehrhardt (Eds.), *Methods of seawater analysis* (pp. 437–444). Wiley-VCH.

Hansen, H. P., & Koroleff, F. (1999). Determination of nutrients. In K. Grasshoff, K. Kremling, & M. Ehrhardt (Eds.), *Methods of seawater analysis* (pp. 159–228). Wiley-VCH.., pp. Weinheim, Germany.

He, Q., Zhang, K., Wu, S., Zhao, Q., Wang, X., Shen, Z., et al. (2020). Real-Time GNSS-derived PWV for typhoon characterizations: A case study for super Typhoon Mangkhut in Hong Kong. *Remote Sensing*, *12*(1). https://doi.org/10.3390/RS12010104

He, X., Xu, D., Bai, Y., Pan, D., Chen, C.-T. A., Chen, X., & Gong, F. (2016). Eddy-entrained Pearl River plume into the oligotrophic basin of the South China Sea. *Continental Shelf Research*, *124*, 117–124. https://doi.org/10.1016/j.csr.2016.06.003

HELCOM. (2014). *Manual for marine monitoring in the COMBINE programme of HELCOM*.

Hu, J., Kawamura, H., Hong, H., & Qi, Y. (2000). A review on the currents in the South China Sea: Seasonal circulation, South China Sea warm current and Kuroshio intrusion. *Journal of Oceanography*, *56*(6), 607–624. https://doi.org/10.1023/A:1011117531252

Huang, Q.-z., Wang, W.-z., Li, Y. S., & Li, C. W. (1994). Current characteristics of the South China Sea. In Z. Di, L. Yuan-Bo, & Z. Cheng-Kui (Eds.), *Oceanology of China seas* (pp. 39–47). Springer Netherlands. https://doi.org/10.1007/978-94-011-0862-1_5

IPCC. (2019). IPCC special report on the ocean and cryosphere in a changing climate. In *Intergovernmental panel on climate change* (p. 755). In press.

Johnston, T. M. S., Rudnick, D. L., Brizuela, N., & Moum, J. N. (2020). Advection by the north equatorial current of a cold wake due to multiple typhoons in the Western Pacific: Measurements from a profiling float array. *Journal of Geophysical Research: Oceans*, *125*(4). https://doi.org/10.1029/2019JC015534

Li, D., Gan, J., Hui, R., Liu, Z., Yu, L., Lu, Z., & Dai, M. (2020). Vortex and biogeochemical dynamics for the hypoxia formation within the coastal transition zone off the Pearl River Estuary. *Journal of Geophysical Research: Oceans*, *125*(8), e2020JC016178. https://doi.org/10.1029/2020JC016178

Liu, S., Li, J., Sun, L., Wang, G., Tang, D., Huang, P., et al. (2020). Basin-wide responses of the South China Sea environment to super typhoon Mangkhut (2018). *The Science of the Total Environment*, *731*, 139093. https://doi.org/10.1016/j.scitotenv.2020.139093

Liu, X., Wang, Q., Liu, C., He, Y., Wang, S., Hou, P., et al. (2020). Wind field reconstruction and analysis of super typhoon Mangkhut (1822). *Journal of Coastal Research*, *99*(sp1), 151–157. https://doi.org/10.2112/SI99-022.1

Lo, H. S., Lee, Y. K., Po, B. H. K., Wong, L. C., Xu, X., Wong, C. F., et al. (2020). Impacts of Typhoon Mangkhut in 2018 on the deposition of marine debris and microplastics on beaches in Hong Kong. *The Science of the Total Environment*, *716*, 137172. https://doi.org/10.1016/j.scitotenv.2020.137172

Pan, S., Shi, J., Gao, H., Guo, X., Yao, X., & Gong, X. (2017). Contributions of physical and biogeochemical processes to phytoplankton biomass enhancement in the surface and subsurface layers during the passage of Typhoon Damrey. *Journal of Geophysical Research: Biogeosciences*, *122*(1), 212–229. https://doi.org/10.1002/2016JG003331

Qiu, D., Zhong, Y., Chen, Y., Tan, Y., Song, X., & Huang, L. (2019). Short-term phytoplankton dynamics during typhoon season in and near the Pearl River Estuary, South China Sea. *Journal of Geophysical Research: Biogeosciences*, *124*(2), 274–292. https://doi.org/10.1029/2018JG004672

Redfield, A. C., Ketchum, B. H., & Richards, F. A. (1963). In M. N. Hill (Ed.), *The influence of organisms on the composition of sea waterThe sea* (pp. 26–77). J. Wiley.

Shaw, P.-T., & Chao, S.-Y. (1994). Surface circulation in the South China Sea. *Deep-Sea Research I*, *41*(11), 1663–1683. https://doi.org/10.1016/0967-0637(94)90067-1

Suzuki, Y., Tanoue, E., & Ito, H. (1992). A high-temperature catalytic oxidation method for the determination of dissolved organic carbon in seawater: Analysis and improvement. *Deep-Sea Research*, *39*(2), 185–198. https://doi.org/10.1016/0198-0149(92)90104-2

Wang, B., Xu, Y., & Bi, B. (2007). Forecasting and warning of tropical cyclones in China. *Data Science Journal*, *6*, S723–S737. https://doi.org/10.2481/dsj.6.s723

Wang, D., Shu, Y., Xue, H., Hu, J., Chen, J., Zhuang, W., et al. (2014). Relative contributions of local wind and topography to the coastal upwelling intensity in the northern South China Sea. *Journal of Geophysical Research: Oceans*, *119*(4), 2550–2567. https://doi.org/10.1002/2013JC009172

Waniek, J. J., Frazão, H. C., Schuffenhauer, I., & Mars, R. (2021). *Physical oceanography during the cruise Hai Yang Di Zhi Shi Hao in South China Sea in September 2018*. PANGAEA. https://doi.org/10.1594/PANGAEA.936352

Waniek, J. J., Kuss, J., Frazão, H. C., Schulz-Bull, D., Jeschek, J., Sadkowiak, B., et al. (2021). *Hydrochemistry measured on water bottle samples during the cruise Hai Yang Di Zhi Shi Hao in south China Sea in September 2018*. PANGAEA. https://doi.org/10.1594/PANGAEA.936096

Winkler, L. W. (1888). Die Bestimmung des im Wasser gelösten Sauerstoffes. *Berichte der Deutschen Chemischen Gesellschaft*, *21*, 2843–2854. https://doi.org/10.1002/cber.188802102122

Wyrtki, K. (1961). *Physical oceanography of the Southeast Asian waters*. The University of California, Scripps Institution of Oceanography.

Ying, M., Zhang, W., Yu, H., Lu, X., Feng, J., Fan, Y., et al. (2014). An overview of the China meteorological administration tropical cyclone database. *Journal of Atmospheric and Oceanic Technology*, *31*(2), 287–301. https://doi.org/10.1175/JTECH-D-12-00119.1

Yu, P., Wang, Z. A., Churchill, J., Zheng, M., Pan, J., Bai, Y., & Liang, C. (2020). Effects of typhoons on surface seawater pCO_2 and air-sea CO_2 fluxes in the northern South China Sea. *Journal of Geophysical Research: Oceans*, *125*(8), e2020JC016258. https://doi.org/10.1029/2020JC016258

Zhao, H., & Wang, Y. (2018). Phytoplankton increases induced by tropical cyclones in the South China Sea during 1998–2015. *Journal of Geophysical Research: Oceans*, *123*(4), 2903–2920. https://doi.org/10.1002/2017JC013549

Zheng, G. M., & Tang, D.-L. (2007). Offshore and nearshore chlorophyll increases induced by typhoon winds and subsequent terrestrial rainwater runoff. *Marine Ecology Progress Series*, *333*, 61–74. https://doi.org/10.3354/meps333061